paper on methodology

Protocol for the preparation of a segmental linear polyacrylamide gradient gel: simultaneous determination of Lp[a], LDL, and HDL particle sizes

Xianzhou Li, Wendy Innis-Whitehouse, W. Virgil Brown, and Ngoc-Anh Le[1]

Division of Arteriosclerosis and Lipid Metabolism, Department of Medicine, Emory University School of Medicine, 1639 Pierce Drive, Atlanta, GA 30322

Abstract We describe in this report a protocol for the preparation of a polyacrylamide gel system (S-GGE 2.8/8.30) that consists of two linear gradients designed for the simultaneous determination of the diameters of LDL and HDL from whole plasma. The lower gel consists of an 8–30% linear gradient which is optimum for the resolution of HDL subfractions and the upper gel consists of a 2–8% linear gradient to allow for the resolution of LDL and larger lipoprotein fractions such as Lp[a] and small VLDL. In contrast to other non-denaturing gradient gel systems which are based on protein staining, the present system uses lipid stain to specifically identify lipoproteins. This approach also allows the plasma to be pre-stained with immediate visualization of the lipid bands being possible at the completion of the electrophoretic run. Using commercially available gel casting equipment, the present gradient gel system can accommodate up to 21 lanes per gel. The inter-run and intra-run coefficients of variation for LDL particle size are 0.47 and 0.16%, respectively. The inter- and intra-run CVs for Lp[a] particle size are 0.92% and 0.89%, respectively. The inter-run and intra-run coefficients of variation for HDL_2 and HDL_3 particle size are 1.36% and 3.23%, respectively.—**Li, X., W. Innis-Whitehouse, W. V. Brown, and N-A. Le.** Protocol for the preparation of a segmental linear polyacrylamide gradient gel: simultaneous determination of Lp[a], LDL, and HDL particle sizes. *J. Lipid Res.* 1997. **38:** 2603–2614.

Supplementary key words lipid staining • gradient gel electrophoresis

Sixty to 75% of the cholesterol in blood is associated with low density lipoproteins which consist of a non-homogeneous mixture of spherical particles ranging widely in particle size (23–28 nm), buoyant density, and chemical composition (1, 2). Using a non-denaturing 2–16% polyacrylamide gradient gel electrophoresis, Austin and Krauss (3) have noted that individuals with a high-risk lipid profile were most likely to have primarily small, dense low density lipoprotein (LDL) particles. In a case-control study of men and women with documented myocardial infarction (MI), Austin et al. (4) reported that LDL phenotype B, the LDL subclass pattern characterized by a preponderance of small dense LDL particles, was associated with a 3-fold increased risk of MI. This association remained significant after adjustment for age, sex, and relative weight. It has also been suggested that there may be a major genetic determinant for this LDL phenotype (5). Whether or not the relationship between LDL phenotype and coronary artery disease (CAD) is independent of other risk factors such as LDLc, HDLc (6), or triglyceride (TRIG) (7) is still unclear.

High density lipoproteins (HDL) are responsible for the reverse transport of cholesterol from peripheral tissues back to the liver. Data from Cheung et al. (8) and Johansson et al. (9) suggest that patients with documented CAD may have altered HDL particle size distribution when compared to that observed in non-CAD controls. In these studies, the heterogeneity of plasma HDL was assessed using a non-denaturing 4–30% polyacrylamide gradient gel first described by Blanche et al. (10).

A major impediment to large prospective studies of lipoprotein particle size distribution has been the unavailability of an efficient and reproducible method that can allow the determination of particle diameters for cholesterol-rich lipoproteins. High quality pre-cast

Abbreviations: S-GGE 2.8/8.30, segmental gradient gel electrophoresis with a 2–8% and an 8–30% gradient; TRIG, triglycerides; CHOL, cholesterol; VLDL, very low density lipoproteins; IDL, intermediate density lipoproteins; LDL, low density lipoproteins; HDL, high density lipoproteins; HDLc, HDL-cholesterol; LpA-I, apoA-I-containing lipoproteins; LpA-I/A-II, lipoproteins containing both apoA-I and apoA-II; LpB, apoB-containing lipoproteins; LDLc, LDL-cholesterol.

[1]To whom correspondence should be addressed.

gradient gels used in the earlier studies are no longer available commercially. Rainwater et al. (11) have reported a procedure for the preparation of a 4–30% gradient gel that provides estimates of HDL particle size comparable to those obtained with the PAA 4/30 (Pharmacia). In this gradient, however, LDL and larger lipoprotein particles tend to accumulate at the top of the gel, prohibiting the determination of particle size of these lipoproteins. A custom-made 2–16% gradient gel was also described by these investigators for the determination of LDL particle size (12). Except for Gambert et al. (13), who used lipid staining to visualize the LDL band, most investigators used Coomassie to stain the gels for protein after the electrophoresis. The use of a protein stain typically requires extensive staining and de-staining procedures for the gels after electrophoresis and special handling of the gels during these steps to maintain gel size and shape before scanning (12). Furthermore, by using a protein stain, many protein bands other than those corresponding to plasma lipoproteins are visible from the electrophoresis of whole plasma.

We have developed a protocol for the casting of a segmental gradient gel that would provide optimal conditions for the simultaneous characterization of LDL (2–8% gradient) and HDL subclasses (8–30% gradient) from whole plasma. Commercial kits available for the preparation of gradient gels can be used for the preparation of this gel. The system described in this report uses a novel layering technique to ensure the formation of a uniform linear gradient across a wide gel that provides up to 21 sample lanes. With the conventional dual-gel electrophoretic chamber, a maximum of 42 samples can be analyzed simultaneously. Another advantage of this protocol is the use of the lipid stain Sudan Black to pre-stain whole plasma, thus allowing the immediate and specific visualization of only lipid-containing particles in plasma without requiring the extensive procedure associated with the staining and de-staining of the gel after electrophoresis. Furthermore, instead of using R_f to relate molecular weight to particle diameter, we took advantage of the unique relationship between acrylamide concentration and pore size to define a concept of gel constant that can be used to calculate particle diameter. This concept is based on the observation of Fawcett and Morris (14) who noted that, for a linear gradient of polyacrylamide, the gel pore size at any point in the gradient is proportional to the concentration of acrylamide at that point and spherical particles cannot migrate through pore sizes that are smaller than their respective diameters (15). Thus, the particle diameter of a lipoprotein band in any lane of the gradient can subsequently be calculated from the gel constant which can be uniquely defined for that gradient based on the position of a number of calibrators of known diameters.

METHODS

Materials and Equipment

Acrylamide was obtained from Sigma Chemicals (A-3553 and M-7279), as were the ammonium persulfate (A-1433) and TEMED (T-9281) and the stain, Sudan Black B (Sigma: S-0395). Ethylene glycol (E178-1) and boric acid (BP 168-500) were purchased from Fisher Scientifics. Tris(hydroxymethyl)aminomethane (EK-1174952) was from VWR Scientifics.

The gel apparatus was purchased from Hoefer and included the SE 650 vertical slab unit, the SG-100 gradient maker, and the PS-1500 power supply. The gradient gel was prepared using the 18 × 8 slab gel unit from Hoefer (SE 6402) with a 3-mm spacer. Two 12-slot sample applicators from Isolabs (GC-50) were adapted for our gel system to optimize sample loading. The gel was scanned using the LKB 222-020 UltroScan XL Laser Densitometer. The principle for the multitrack gradient layering unit developed for these gradient gels is illustrated in **Fig. 1**. In our prototype, the oscillating motion of the dispensing arm was controlled by a platform mixer (Vari-Mix, Thermolyne).

Buffers

Three stock preparations containing high, intermediate, and low concentrations of acrylamide were available: 1) high: 38.4 grams of acrylamide and 1.6 g N,N′-methylene-bis-acrylamide in 100 ml of borate buffer (80 mM boric acid, 90 mM Tris, 3 mM EDTA, pH 8.3) and 2) medium: 10.24 g acrylamide and 0.43 g N,N′-methylene-bis-acrylamide in 100 ml of borate buffer and 3) low: 2.3 g acrylamide and 0.19 g N,N′-methylene-bis-acrylamide in 100 ml of borate buffer. A stock solution of TEMED was prepared by combining 0.6 ml of TEMED and 99.4 ml of the borate buffer. Ammonium persulfate solution (5 mg/ml) was also prepared with the borate buffer.

Preparation of segmental gradient polyacrylamide gels (S-GGE 2.8/8.30)

The segmental polyacrylamide gradient gel (3 mm thick) was poured in two steps using the Hoefer SE 6402 gel maker kit with 18 × 8 cm glass plates and the gradient maker (Hoefer GS100). Each chamber of the gradient maker was filled with a mixture of 6 ml of the appropriate acrylamide concentration, 1 ml of TEMED buffer, and 1 ml of ammonium persulfate solution. For

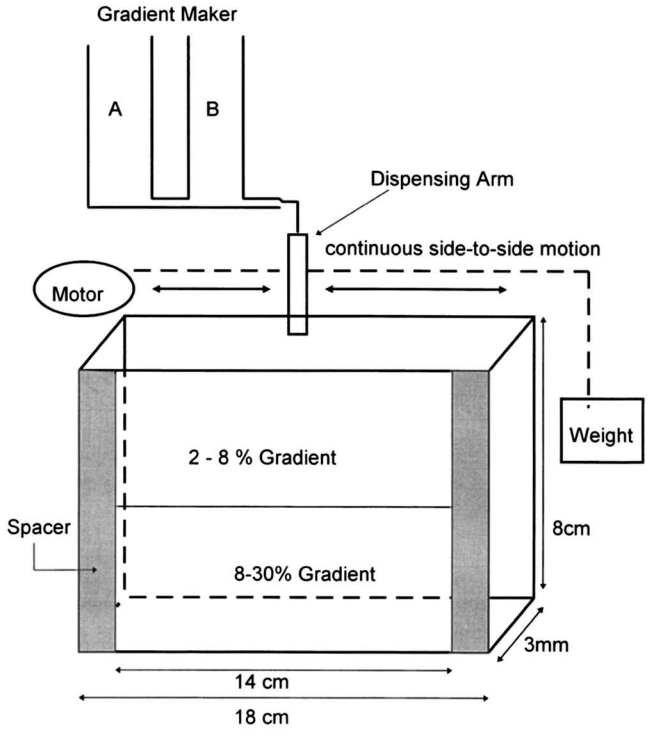

Fig. 1. Schematic of the apparatus for the preparation of linear gradient gel. In this setup, the higher concentration of polyacrylamide is always in chamber B of the gradient maker for both linear gradients. The gel volume for each gradient is approximately 16 ml (7 cm wide by 3.8 cm high and 0.3 cm thick). Parameters that have been optimized for the preparation of the gradient gels include the rate of the side-to-side motion of the dispensing arm and the rate of flow from the dispensing tip as determined by the distance from the bottom of the gradient maker to the tip of the dispensing arm. Variation in one of these parameters must be matched by an appropriate change in the other parameter in order to preserve the quality of the gradient.

the first stage, the two chambers contained the high (chamber B) and medium (chamber A) concentrations of acrylamide to generate the 8–30% gradient. As schematized in Fig. 1, the acrylamide solutions were allowed to flow continuously as the dispensing arm was moved from side to side along the upper rim of the glass plates, thus creating multiple tracks along the glass plates across the width of the gel chamber. This motion (15 side-to-side oscillations/min) ensured the even distribution of the acrylamide solution between the plates over the entire width of the gel (14 cm). The chambers were allowed to empty completely creating the lower gradient gel (approximately 3.8–4 cm in height) which was then allowed to polymerize at room temperature (2 h). The chambers of the gradient makers were subsequently filled with the medium (chamber B, 6 ml) and low (chamber A, 6 ml) concentration acrylamide to form the 2–8% linear gradient gel. To each chamber, 1 ml of TEMED buffer and 1 ml of ammonium persulfate solution were added for a total of 16 ml for both chambers. The quality and reproducibility of the gel is optimal if the rate of gel flow is matched to the appropriate rate of movement of the dispensing arm. The rate of flow is controlled by gravity (18.5 cm in height) with a mean rate of 1.5 ml/min and the dispensing arm moved at a rate of 15 cycles/min.

Electrophoresis

Whole plasma (30 μl) was mixed with 10 μl of a prestaining solution (0.6% Sudan Black B solution in ethylene glycol) prior to application to the gel. After a 2-h incubation period at room temperature, a single load of 10 μl of prestained plasma solution was applied to individual troughs, characteristic of the GA-50 sample applicator (Isolabs). Electrophoresis was performed at room temperature, 50 mA, 80 V for 18–20 h. The lipoprotein bands were scanned at 633 nm using the LKB 222-020 UltroScan XL Laser Densitometer.

Calibration of lipoprotein particle size

Whole plasma from a human donor exhibiting distinct lipoprotein bands corresponding to LDL, Lp[a], HDL_2, and HDL_3 (CHOL = 297, TG = 97, HDLc = 73, and Lp[a] = 29 mg/dL) was run in multiple lanes of each gel. The diameter of the LDL band in this plasma sample was calibrated using a set of in-house LDL calibrators (27.7, 25.3, and 24.2 nm). The diameters for the in-house LDL calibrators had been previously standardized against the calibrator pool ILH containing LDL with diameters of 29.7, 27.1, and 24.7 nm available from Dr. Krauss (Donner Laboratory) as previously reported (16, 17) using PAA 2/16 gels from Isolabs.

As with other gradient gel systems, the diameters of HDL_2 and HDL_3 in the S-GGE 2.8/8.30 gradient gel were determined using the high molecular weight calibrators obtained from Pharmacia (HMW 17-0445-01). For these calibration runs, the gels were stained for protein with Coomassie after electrophoresis to visualize the protein bands corresponding to the molecular weight standards. The high molecular weight calibrators included: thyroglobulin (17.0 nm), ferritin (12.2 nm), catalase (10.4 nm), lactate dehydrogenase (8.4 nm), and albumin (7.1 nm). Frozen aliquots of plasma from this donor were maintained at −80°C (up to 2 years) and included in all subsequent runs as calibrators for the gel. The quality of the calibrators was assessed by the actual position of the bands as well as the values calculated for the gel constant (see below). These aliquots were thawed once for each use and discarded without being re-frozen for later use.

Determination of particle size using the gel constant

From gel chromatography experiments, Fawcett and Morris (14) noted that the pore size (S_{pore}) of polyacrylamide gel varied inversely to the monomer concentration ($T_{gradient}$), i.e.

$$S_{pore} = K_1[1/T_{gradient}] \quad \textit{Eq. 1)}$$

where K_1 denotes the unknown proportionality constant. For a linear gradient, the monomer concentration $T_{gradient}$ of the polyacrylamide at any distance d in the gel is a function of the distance d from the top of the gel, thus

$$T_{gradient} = f(d) \quad \textit{Eq. 2)}$$

The function f will also depend on the range and slope of the gradient. By combining equations 1 and 2, we obtained:

$$S_{pore} = K_1 \times [1/f(d)] \quad \textit{Eq. 3)}$$

When gradient electrophoresis is carried out to completion, spherical particles of uniform size will continue to migrate until they reach a distance in the gradient, $d_{particle}$, where the pore size of the gel matrix becomes so small as to prevent further penetration by the particle. At this point of equilibrium the pore size is approximately equal to the particle size. In other words,

$$S_{particle} = S_{pore} = K_1 \times [1/f(d_{particle})] \quad \textit{Eq. 4)}$$

or

$$C_{gel} = S_{particle} \times f(d_{particle}) = S_{pore} \times f(d_{particle}) \quad \textit{Eq. 5)}$$

By using a calibrator of known particle diameter $S_{calibrator}$ and by measuring the distance $d_{calibrator}$ migrated into the gel of this calibrator, we can calculate the gel constant, C_{gel}, for this particular linear gradient.

$$C_{gel} = S_{calibrator} \times f(d_{calibrator})$$

Using the distances determined by the gel scanner for the bands corresponding to the LDL, Lp[a], HDL_2, and HDL_3 calibrators, we can calculate the gel constants for the upper and lower gels. As the distance $d_{calibrator}$ depents ultimately on the polyacrylamide concentration in the gel gradient, equation 5 would indicate that C_{gel} will depend only on the pore size and should, in theory, be the same independent of the gradient:

$$C_{gel}(nm - \%) = S_{calibrator} \times [L + (d_{calibrator})*(Slope_{gradient})] \quad \textit{Eq. 6)}$$

where $S_{calibrator}$ is the known diameter (nm) of the calibrator; L is the lowest gel concentration for the gradient, i.e., 2% for the 2–8% gradient and 8% for the 8–30% gradient; $d_{calibrator}$ (mm) is the position of the band corresponding to the calibrator from the top of the gradient; $Slope_{gradient}$ is the slope (% per mm) of the gradient, or the difference between the lowest and and the highest gel concentrations (6% for the top gradient and 22% for the bottom gradient) divided by the height of the gel. The actual height of each gradient can be determined by the operator for each gel using the scanner.

2–8% gradient

with Lp[a]

$C_{gel} = 30.40 \times [2 + (9.8)*(6/35)] = 111.863$

with LDL

$C_{gel} = 25.70 \times [2 + (13.7)*(6/35)] = 111.748$

8–30% gradient

with HDL_2

$C_{gel} = 11.80 \times [8 + (38.40-35.0)*(22/37)] = 118.255$

with HDL_3

$C_{gel} = 9.60 \times [8 + (41.70-35.0)*(22/37)] = 115.044$

From this estimate of the gel constant, the diameter $S_{unknown}$ of any particle can be calculated from the distance $d_{unknown}$ from the top of the gel. It should be noted that the densitometer gives the position of the band as referenced to an arbitrary set point (typically, from the edge of the glass plate) and the distance to the top of the gradient must be subtracted to obtain the true distance of migration into the gel. Furthermore, for the lower gradient gel, the actual height of the upper gel must also be subtracted.

$$S_{unknown} = C_{gel}/f(d_{unknown})$$

With each gel, the calibrator plasma containing Lp[a], LDL, HDL_2, and HDL_3 of known particle diameters was always applied in three separate lanes including the two outside lanes and one toward the center of the gel. From the previously determined diameters of Lp[a] and LDL in the calibrator plasma, six separate estimates (2 calibrators × 3 lanes) were obtained for the gel constant of the 2–8% gradient. The mean value was used to determine the diameters of LDL and Lp[a] in the unknown samples. Similarly, the diameters of HDL_2 and HDL_3 in the calibrator plasma allowed the calculation of six estimates for the gel constant corresponding to the 8–30% gel gradient and the mean value was used in calculating the HDL particle diameter.

Lipoprotein isolation

To examine the characteristics of the different class of lipoproteins in this system, individual fractions were isolated by ultracentrifugation from freshly collected plasma. VLDL was recovered in the supernate of the d 1.006 g/ml spin (24-h spin at 39,000 rpm and 10°C) using the SW 40 swinging bucket rotor (Beckman Instruments, Palo Alto, CA). LDL was recovered in the density range of 1.019–1.063 g/ml by sequential ultra-

centrifugation. Lp[a] was isolated by density ultracentrifugation using a modification of the method reported by Fless, ZumMallen, and Scanu (18). In brief 1 ml of plasma was adjusted to a density of 1.050 g/ml using solid KBr and layered with 12 ml of a 1.040 g/ml density solution. Ultracentrifugation was performed at 35,000 rpm for 15 h (10°C) using the SW 40 swinging bucket rotor. The fraction corresponding to Lp[a] was removed by careful aspiration and confirmed by ELISA.

In order to compare our estimates obtained for HDL-sized particles with this new procedure, we used LpA-I and LpA-II/A-II fractions that had been isolated by immunoaffinity chromatography and generously donated by Dr. M. Cheung of the Northwest Lipid Research Laboratory (8). The diameters of the major protein fractions in these HDL subclasses had been determined using the 4–30% gel available from Alamo Gels, Inc (San Antonio, TX). By using these purified HDL subfractions to compare the estimates of particle diameters obtained by the two gels we can be sure that only peaks corresponding to HDL proteins are visualized after staining with Coomassie.

RESULTS

Reproducibility of the S-GGE 2.8/8.30 for lipoprotein particle diameter

Figure 2A illustrates the reproducibility of the linear gradient across the 21 lanes of the gel as demonstrated by identical distances of migration across all lanes for all four major lipoprotein bands. Figure 2B presents the actual particle diameters obtained for LDL and Lp[a] when the calibrator plasma was applied in multiple lanes of five different gels. Only 9.4% (3/32) of the individual particle diameter estimates for LDL were outside 1 SD of the mean and none were outside 2 SD. For Lp[a], 12.5% (4 out of 32 lanes) of the particle diameter estimates from five separate gels were outside 1 SD of the mean. None were outside 2 SD. For the HDL subfractions, 18.8% (6 out of 32 lanes) were outside 1 SD and 6.2% (2 out of 32) were outside 2 SD (Fig. 2C). **Table 1** presents the mean values and fractional standard deviation (100 × SD/mean) for the distance from the top and for the calculated particle diameter for Lp[a], LDL, HDL_2, and HDL_3 from 16 lanes on the same gel (within run) as well as values from 65 different gels (between runs).

The reproducibility of the gel constants (mean ± SEM for the most recent series of 100 gels) was obtained for both the 2–8% (C_{gel} = 113.5 ± 0.45) and the 8–30% linear gradients (C_{gel} = 116.43 ± 0.28). There was no statistical difference between the two estimates for the C_{gel} from the lower and upper gradient gels as assessed by unpaired *t*-test. These empirical results further support the earlier observation that the pore size at any point in a linear gradient is defined solely by the gel concentration, independent of the range of the gradient prepared.

In order to examine the effect of the pre-staining procedure on the electrophoretic mobility of the lipoproteins, whole plasma aliquots from a single donor were incubated in the staining solution for 15 min, 30 min, 1 h, and 2 h at room temperature and electrophoresed in adjacent lanes. As shown in **Fig. 3A**, there was no change in the position of any bands corresponding to the four major lipoprotein fractions. **Table 2** presents the actual particle diameters for six separate incubations at 15 min, 1 h, and 2 h for a freshly collected plasma sample that displays all four major lipoprotein bands. There was no statistical difference in particle size with the different incubation times.

Figure 3B illustrates the reproducibility of the position of LDL bands as different concentrations of LDLc were applied. With the present protocol for pre-staining and electrophoresis, particle size determination for LDL can be determined from a sample with an LDLc concentration of 40 mg/dL. While there appeared to be a dose-dependence between LDLc and the intensity of the stained LDL bands, we were not able to establish a reliable standard curve between the areas under the LDL peaks as determined from the densitometer and the concentrations of LDL when plasma samples from different donors were analyzed. This is in contrast to the reported data obtained with protein staining. Differences in the lipid composition of LDL among individuals could account for the variability in the stain intensity for different preparations of LDL.

In contrast to the sharp bands characteristic of LDL, small VLDL can be shown to have significantly broader peaks which are poorly stained (Fig. 3C). For this experiment, VLDL from a normotriglyceridemic donor (CHOL = 195, TG = 80, HDLc = 56, and Lp[a] < 0.1 mg/dL) was isolated by ultracentrifugation using the SW40 swinging bucket at density d < 1.006 g/ml. In contrast to the band corresponding to 40 mg/dL of LDLc (lane 4, Fig. 3B), the band corresponding to 50 mg/dL of VLDL-cholesterol (lane 3, Fig. 3C) was barely visible under identical staining conditions. As shown, the band corresponding to VLDL from this normotriglyceridemic individual was slightly larger than Lp[a] in our calibrator (lane S) and was significantly more heterogeneous as indicated by the broadness of stained band. In our hands, VLDL isolated by ultracentrifugation of whole plasma obtained from individuals with fasting TG of 350 mg/dL or greater can be visualized as a dark stain at the top of 2% gel, suggesting that these particles were too large to

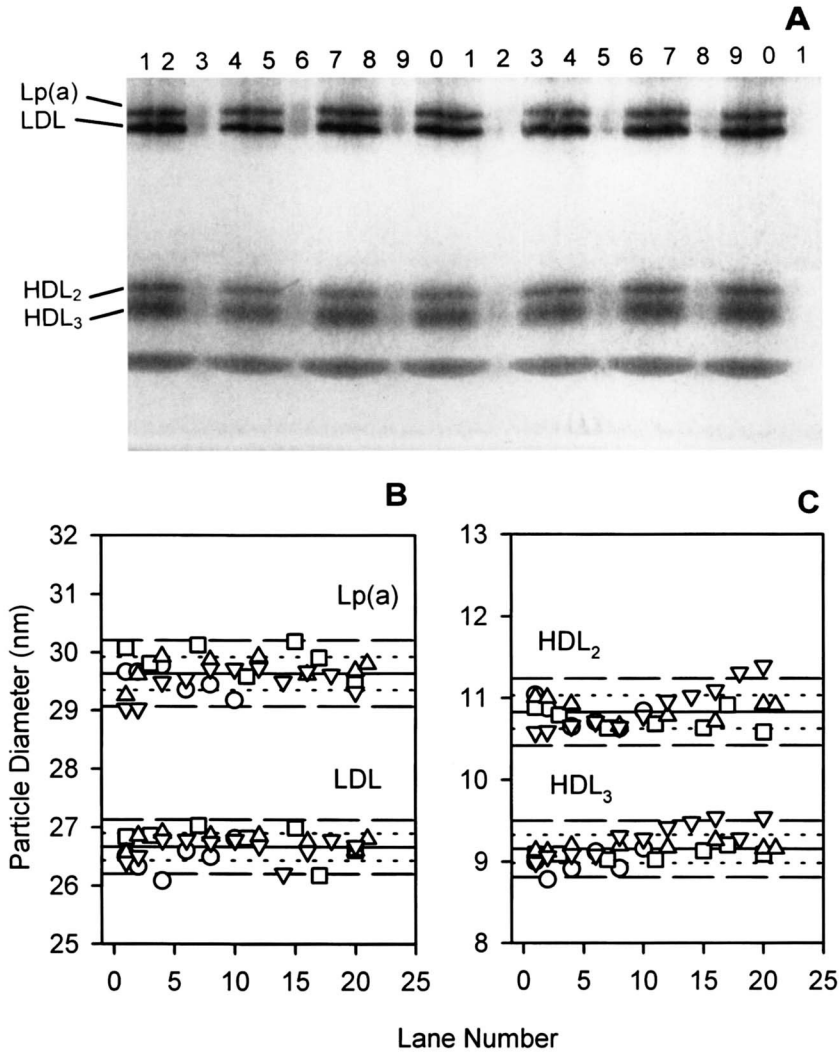

Fig. 2. Reproducibility of lipoprotein particle size determinations. Actual photograph (panel A) of a gradient gel with the same plasma sample (CHOL = 279, TG = 65, HDLc = 65 and Lp[a] = 175 mg/dL being applied to 17 of the 21 available lanes. Aliquots of this plasma sample were also applied to different lanes (x-axis) for five different gels (different symbols) over a 2-week period. The calculated particle diameters (nm) are plotted on the vertical axis as function of lane number (horizontal axis) for each gel and the different symbols represent results from different gels. The mean diameter (—), 1 SD range (---) and 2 SD range (——) are presented for LDL and Lp[a] particle diameter (panel B) as well as for HDL_2 and HDL_3 (panel C).

TABLE 1. Reproducibility of the distance of migration into the gel and diameter of the major classes of lipoproteins in whole plasma

	Within-Run (n = 16 lanes)		Between-Run (n = 65 gels)	
Lipoprotein	Distance	Diameter	Distance	Diameter
	mm	*nm*	*mm*	*nm*
Lp[a]	9.80 ± 2.76	30.70 ± 0.92	9.80 ± 2.96	30.30 ± 0.89
LDL	13.70 ± 1.68	25.70 ± 0.77	13.70 ± 2.76	25.90 ± 1.16
HDL_2	38.70 ± 1.55	11.80 ± 1.36	38.80 ± 2.09	12.10 ± 3.23
HDL_3	71.70 ± 1.37	9.60 ± 1.25	72.70 ± 2.11	9.70 ± 2.58

Values are given as mean ± SD. The migration distance is calculated as the position of the peak as printed by the gel scanner program minus the position of the top of the respective gel gradient.

enter the gel matrix. Using the value of gel constant calculated for the 2–8% gel and equation 6, we would predict that only particles with diameter less than 55 nm would be able to enter the gradient.

Identification of Lp[a]

The identity of the Lp[a] band was confirmed by several approaches. First, the stain characteristics of the Lp[a] band are different from those of VLDL (Fig. 3C). The Lp[a] band is sharper and more comparable to that of LDL than to that of VLDL. Second, isolated fractions of Lp[a] can be shown to correspond to distinct peaks upon electrophoresis in the S-GGE 2.8/8.30

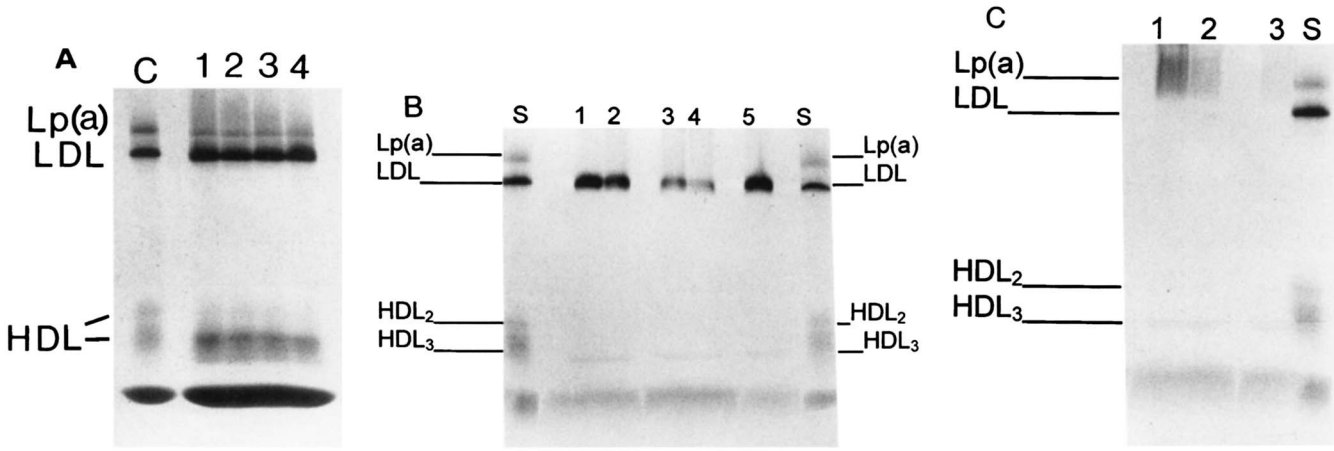

Fig. 3. Conditions for optimal lipoprotein bands on the S-GGE 2.8/8.30 gel. In all of these panels, S indicates the lane to which the Standard (calibrator) sample was applied. Panel A: By varying the incubation period for pre-staining of whole plasma from 120 min (lane 1), 60 min (lane 2), 30 min (lane 3), to 15 min (lane 4) we can show that there was no effect on the position of the Lp[a], LDL, HDL_2, and HDL_3 bands. Panel B: The position of the LDL band was not affected by the concentration of LDLc in the 10 μl of sample applied to the lane. A concentrated preparation of LDL (LDLc = 270 mg/dL, lane 5) isolated by ultracentrifugation was dialyzed against normal saline (d 1.006 g/ml and 0.01% EDTA) and diluted with d 1.006 g/ml solution containing 0.01% EDTA to various concentrations of cholesterol ranging from 160 (lane 1), 80 (lane 2), 50 (lane 3), to 40 (lane 4) mg/dL. All diluted samples were pre-stained by incubation at room temperature for 2 h. Panel C: The application of comparable concentrations of cholesterol in the form of VLDL resulted in considerably broader bands which are less intensely stained as compared to LDL and Lp[a]. VLDL was isolated by ultracentrifugation and applied at cholesterol concentrations of 100 mg/dL (lane 1, ~530 mg/dL of TG), 50 mg/dL (lane 2, 265 mg/dL of TG) and 25 mg/dL (lane 3, 133 mg/dL of TG).

gel with migration distance identical to the corresponding peaks obtained with whole plasma (**Fig. 4**). And third, analysis of postprandial plasma samples from an individual demonstrated that the peak corresponding to Lp[a] was unchanged while the area under the peak corresponding to remnants increased at 2 h postprandially before returning to fasting level after 10 h (**Fig. 5**).

Figure 4A illustrates actual gel scans for a plasma sample with a high concentration of Lp[a]. In Fig. 4B, we present the gel scan of a partially purified Lp[a] isolated by density gradient ultracentrifugation using the SW40 swinging bucket as previously described by Fless et al. (18). The position of the Lp[a] peak was 28.20 mm in whole plasma as compared to 28.52 mm for the isolated Lp[a] from the edge of the plate. This corresponds to a distance of 8.2–8.5 mm from the top of the gel gradient. The gel scan in Fig. 4C illustrates a single peak for LDL isolated by ultracentrifugation in the density range 1.020–1.063 g/ml from the same plasma. In all samples with Lp[a] concentrations of 35 mg/dL or greater as determined by ELISA, we have consistently been able to visualize a band at approximately 8.2–8.75 mm from the top of the gel corresponding to a particle diameter in the range of 27 to 30 nm.

To further demonstrate the ability of the gel to resolve small VLDL and remnants from Lp[a], we examined non-fasting plasma from an individual with a distinct Lp[a] band present in fasting plasma (Fig. 5A). As shown in Fig. 5A, a distinct peak corresponding to Lp[a] was noted that was slightly larger than LDL and a subpopulation of even larger particles appeared as a shoulder (peak 1) to the left of the Lp[a] peak. Peak 1 was not visible in the gel scans from the plasma of most individuals with normal TG levels (<100 mg/dL, Fig. 4). Postprandial plasma samples collected after the consumption of a standardized liquid test meal containing fat and cholesterol (19, 20) were subjected to electrophoresis (Fig. 5 B–D). At 2 and 4 h after the test meal, when postprandial plasma TG were expected to increase, this shoulder associated with larger lipoprotein particles clearly became a distinct peak (peak 1) with increasing areas (Fig. 5B and C). The position of

TABLE 2. Effect of the duration of the pre-incubation period with the staining solution on lipoprotein particle diameters

	Incubation Time		
Lipoprotein	15 min	1 h	2 h
		nm	
Lp[a]	28.42 ± 0.12	28.30 ± 0.07	28.30 ± 0.17
LDL	25.77 ± 0.22	25.65 ± 0.17	25.77 ± 0.12
HDL_2	11.62 ± 0.06	11.68 ± 0.14	11.67 ± 0.12
HDL_3	9.55 ± 0.12	9.63 ± 0.17	9.72 ± 0.06

Values are given as mean ± SD. For each time period, the sample was incubated in six separate aliquots and analyzed in six separate lanes. All samples were electrophoresed in the same gel.

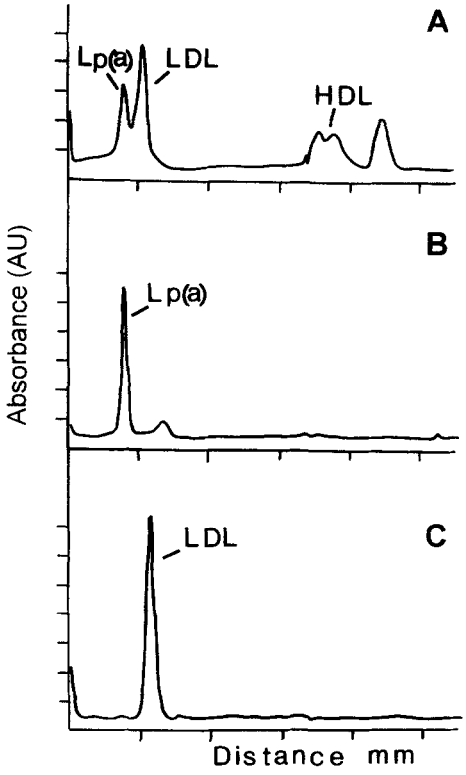

Fig. 4. Gel scans for whole plasma, isolated Lp[a], and isolated LDL. Plasma from a healthy normal control woman (CHOL = 279, TG = 65, HDLc = 65, and Lp[a] = 175 mg/dL) was used for this experiment. Panel A: Two sharp and distinct peaks can be visualized corresponding to lipoprotein particles with diameters of 23 nm or greater. In view of the low plasma TG and high Lp[a] levels in this individual, we postulated that this peak of larger diameter corresponded to Lpl[a]. Panel B: By density gradient ultracentrifugation, a fraction enriched in Lp[a] was isolated and confirmed by ELISA. Upon electrophoresis, this fraction exhibited a major band at the same position as that designated Lp[a] when whole plasma was used. There was a minor peak of small LDL which can be visualized. This would be consistent with contamination by LDL of the Lp[a] fraction which was isolated at a density higher than plasma LDL. Panel C: LDL isolated in the density range 1.020–1.063 g/ml from the same plasma exhibited a single peak corresponding to the major LDL peak seen with whole plasma.

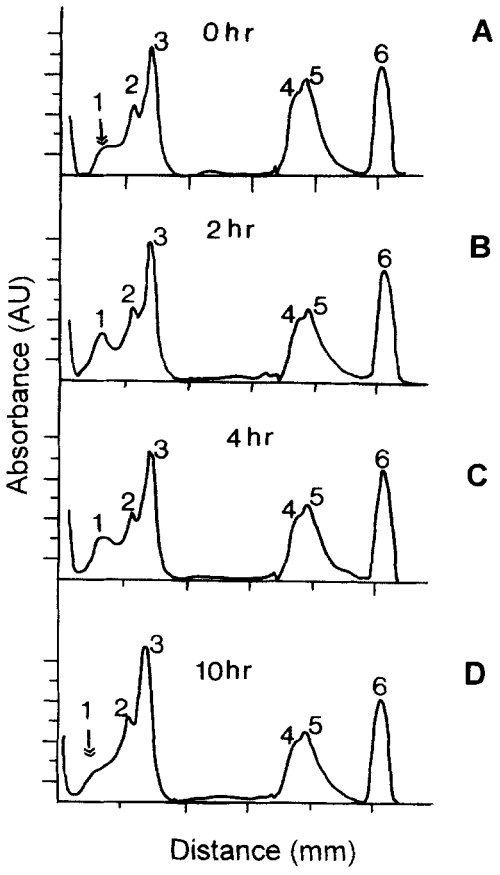

Fig. 5. *Gel scans of whole plasma samples obtained at different* times after the consumption of a fat-containing meal. Panel A: Analysis of fasting plasma from a female patient with documented CAD (Lp[a] = 85, CHOL = 175, TG = 125, HDLc = 79 mg/dL). In addition to the peaks corresponding to Lp[a] (peak 2), LDL (peak 3), HDL_2 (peak 4), HDL_3 (peak 5), and albumin (peak 6), this sample had a prominent shoulder (peak 1) to the left of the Lp[a] peak suggestive of the presence of larger lipoproteins. This shoulder became a well-defined peak at 2 h (panel B) and 4 h (panel C) after the consumption of a single fat-containing meal (see Ref. 19 and 20). In panel D, after 10 h, peak 1 became more of a shoulder to the left of the Lp[a] peak as was the case with the fasting plasma sample. We believe that this broad peak larger than Lp[a] represents TG-rich remnants. The diameter of peak 1 is estimated at 36.7 nm with a range of 32 to 39 nm in different samples.

this band, i.e., the diameter of this lipoprotein fraction, is not changed in postprandial plasma. By 10 h after the test meal, as plasma TG returned to fasting level, this band of larger lipoprotein particles was reduced back to a shoulder to the left of the Lp[a] peak (Fig. 5D). The particle diameter corresponding to this peak is estimated to be 36.7 nm. We postulate that this peak of larger lipoproteins corresponded to TG-rich lipoproteins and their remnants which were generated during postprandial lipemia. This shoulder is demonstrable in only a subset of the individuals studied with the oral fat load and its presence does not appear to be associated with fasting TG levels. Additional experiments are ongoing to further characterize the nature of this lipoprotein peak. It is clear, however, that the sharp band in the size range from 27 to 30 nm must correspond to Lp[a] and not to IDL or other TG-rich remnant lipoproteins which would typically have larger diameters ranging from 33.5 to 39 nm.

HDL particle size: comparison with SFBR 3/31 gel

In order to compare the diameters of HDL particles obtained with our gel system and the conventional

Pharmacia PAA 4/30 gel, we examined LpA-I and LpA-I/A-II fractions isolated by immunoaffinity chromatography (8). These lipoprotein fractions were kindly provided by Dr. Marian Cheung (Northwest Lipid Research Laboratory, University of Seattle, Seattle, WA) and the corresponding diameters were determined using the 3–31% gels (SFBR 3/31, Alamo Gels, Inc., San Antonio, TX) after protein staining. **Figure 6A** illustrates the lipid-stained bands obtained for whole plasma, LpB, LpA-I, and LpA-I/A-II for one individual. In contrast to the protein-stained gels (8, 9), only one or two major bands could be visualized with the lipid stain. For most samples, two lipid-rich bands can always be identified for LpA-I and only one for LpA-I/A-II. Only the major bands with the greatest area under the peak based on the protein stain were selected in this comparison. The two estimates of HDL particle diameters for LpA-I and LpA-I/A-II from 11 individuals were highly correlated (r = 0.978 for a total of 37 peaks). We used this linear regression equation to calculate the adjusted particle diameters of the HDL_2 and HDL_3 in our calibrator. A new gel constant was derived using these adjusted diameters and Fig. 6B illustrated the correlation between the particle diameters for HDL subfractions determined on the S-GGE 2.8/8.30 using the gel constant approach and the values obtained by Dr. Cheung using the SFBR 3/31 gel and the R_f approach. The slope of the linear regression was 0.948 with an intercept of 0.4 nm (r = 0.97).

Effect of sample storage on LDL and Lp[a] particle diameter

Figure 7 illustrates the reproducibility of lipoprotein particle size between fresh samples and frozen samples from a group of 52 individuals including normolipidemic controls and subjects with varying degrees of hyperlipidemia. Fresh plasma samples were analyzed as they were available (within 7 h of collection) using as many as 20 separate gels. Frozen samples were analyzed at the end of an 8-month storage period using four separate gels within a 2-week period. The mean (±SD) LDL particle diameter for the group was 25.7 nm (±0.807) based on the analysis of freshly isolated plasma and 25.3 nm (±0.693) when analyzed from frozen plasma samples. There was no statistically significant difference between the two measurements by two-tailed paired t-test. The mean (±SD) ratio of LDL diameter between the fresh and the frozen estimate was 1.0077 (±0.028). In 26.9% (17 of 51) of the samples, the ratio of the two estimates of LDL particle diameters (fresh vs. frozen) was greater than 1.033 (outside 1 SD) following a single freeze-thaw cycle. For 7.7% of the plasma samples (7 of 52), the ratio of the size estimates for LDL was greater than 1.06 (outside 2 SD) following a single freeze-thaw cycle. One third of the samples (16 of 52) were actually stored for 12 months prior to re-analysis. As there were no differences in the estimates for particle diameter with

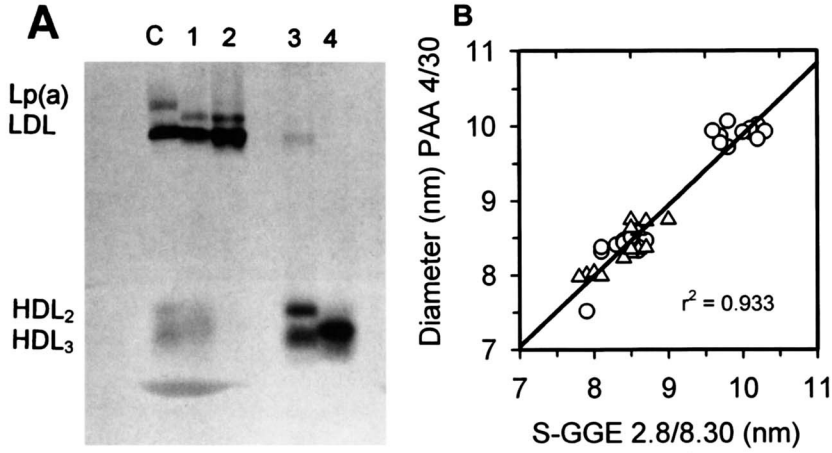

Fig. 6. Comparison of HDL particle size with the SFBR 3/31 gel system. Panel A: Photograph of a gradient gel depicting the calibrator (lane 1), whole plasma (lane 2), LpB (lane 3), LpA-I (lane 7) and LpA-I/A-II (lane 5) for one subject. The band in lane 7 identified in the size range of plasma LDL does not contain apoB as determined by ELISA and can be shown by FPLC to contain phospholipids, cholesteryl esters, cholesterol, apoE, and apoCs (data not shown). Panel B: Correlation between HDL diameters determined by protein staining using the SBFR 3/31 gel from Alamo Gels Inc. and by lipid staining using the S-GGE 2.8/8.30 gel after the diameters of the HDL calibrators were adjusted to be comparable with the values reported by Northwest Lipid Research Laboratory. The triangles (△) correspond to peaks identified from LpA-I fractions and the circles (○) indicate peaks identified from LpA-I/LpA-II fractions.

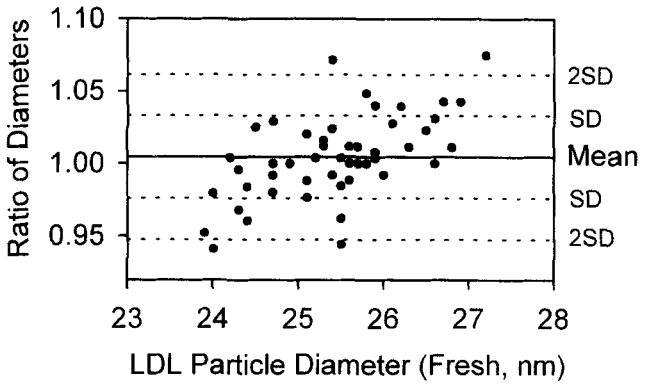

Fig. 7. Effect of sample storage on LDL particle diameter: Plasma samples from 51 subjects including normolipidemic controls and patients with various forms of dyslipidemia were electrophoresed fresh (within 7 h of sample collection) and after storage at −80°C (3–12 months in cryovials without any additives). No statistically significant difference was found between the two estimates by two-tailed paired *t*-test. The ratio of the two estimates of LDL particle diameters (Fresh/Frozen) is plotted as a function of LDL particle diameter determined from freshly isolated plasma. The mean ratio (—), 1 SD (---), and 2 SD lines (— —) are also plotted. The variability in the ratio reflects the combined effect of sample storage and gel reproducibility.

longer storage, results from these samples were included in the final analysis.

DISCUSSION

There is an increased interest in the potential role of LDL particle size as an independent risk factor for premature CAD (3–7). Austin et al. (3, 5) presented data which suggested that LDL subclass patterns may be an inheritable trait. Other investigators would suggest that LDL particle size reflects the metabolism of TG-rich lipoproteins (6, 7). The particle diameters of HDL subclasses are also believed to reflect differences in the metabolism of HDL as modulated by lipid transfer protein (9, 21) and may be associated with risk for CAD (8, 9). The lack of a reliable source of high quality nondenaturing gradient gels has hampered this research. In the development of an efficient gradient gel system for the determination of lipoprotein particle diameter, we emphasized the need for *1*) a way to standardize the gradient, *2*) a system capable of handling more than six samples per gel, *3*) a system that can allow the simultaneous determination of LDL and HDL particle size, and *4*) a system that allows the immediate visualization of the bands without time-consuming staining and destaining procedures.

In the present report we have described a protocol for the preparation of a gradient gel system consisting of two linear gradients, an 8–30% gradient for particles in the range of HDL and a 2–8% gradient for LDL and larger lipoprotein particles. The present system offers several advantages over existing systems previously described in the literature. Using commonly available gel casting equipment and conventional electrophoretic supplies, this protocol allows the reproducible preparation of gradient gels that can accommodate up to 21 samples per gel, or 42 samples per run with a dual-gel electrophoretic chamber. The protocol allows the application of pre-stained plasma samples and the gel can be scanned for particle size immediately at the end of the electrophoretic procedure. Elimination of the extensive staining and de-staining steps after electrophoresis should also minimize the need to handle the gel, preventing any artifact that these steps may introduce. More importantly, the use of a lipid stain allows the specific visualization of only the lipoprotein fractions present in whole plasma.

Several technical aspects of the gel preparation are described to ensure the quality of the gel gradients. In the casting of the typical gradient gels, the polyacrylamide solutions are commonly allowed to flow into the gel chamber from a stationary dispensing line (11) which is typically placed at the center of the gel. However, as the polyacrylamide solution flows from the dispensing tip to the sides of the plate, a secondary gradient is formed across the width of the gel resulting in lower gel concentrations toward the edges. In order to reduce this diffusion effect, only narrow gels with 6–8 lanes across have been available to date. The multitrack and continuous layering technique (Fig. 1) is designed to counter the problems of uneven gradients and disturbances in the process of gel making. With the present system, the side-to-side movement of the dispensing tip ensures even distribution of the polyacrylamide solutions across the entire width of the gel chamber. Multiple tracks of gel solution can be visualized across the width of the gel chamber as the uniform gradient is formed. While crude, the use of the Vari-Mix platform mixer as the motor for the dispensing arm in conjunction with flow rate controlled by gravity (instead of variable-rate diffusion pumps) should allow this protocol to be reproduced at a very reasonable cost. This oscillating delivery scheme is also critical for the reproducible preparation of thicker gels (3 mm) that will be stable at lower acrylamide concentrations (as low as 2%). This increased stability at lower polyacrylamide concentrations is critical for resolving particles larger than LDL such as Lp[a] and TG-rich lipoproteins. However, one disadvantage of these thicker gels is the tendency for the applied samples to diffuse between the glass plates and the gel itself during the first

hour of the electrophoresis. This typically results in faint and blurred bands for the lipoprotein classes. To overcome this problem, we recommend the use of a special sample applicator (GC-50, Isolabs) which is constructed as a series of enclosed troughs ideal for sample loading.

While most gradient gel systems require extensive and time-consuming steps for the staining and de-staining of the gel after the completion of the electrophoresis (7, 11, 15), our protocol uses pre-stained plasma samples (18) and allows immediate visualization of the bands. We have demonstrated that pre-incubation of whole plasma or isolated LDL fractions with the lipid staining solution for up to 2 h at room temperature did not affect the size of LDL, Lp[a], HDL_2, and HDL_3 as assessed by the distance of migration into the gel.

Depending on the composition and concentration of the lipoprotein classes, distinction between Lp[a] and small VLDL or IDL may not be possible by particle size alone. As illustrated in the figures presented here, qualitative differences can be noted between bands corresponding to Lp[a] and those corresponding to remnants of TG-rich lipoproteins (Fig. 3C). The band corresponding to Lp[a] tends to be sharp, and, depending on the Lp[a] concentration, the intensity of this band may be comparable to that observed for LDL (Fig. 2). On the other hand, staining of TG-rich VLDL is significantly less intense, in spite of comparable cholesterol contents (Fig. 3C, lanes 1–3). This ability to distinguish between Lp[a] and TG-rich remnants may be unique to the use of the lipid stain and may not be possible with protein stain as the protein concentration in these lipoprotein fractions is typically lower.

Other evidence in support of the identification of the band in the range of 27–30 nm to be Lp[a] is the characteristic diffuse appearance of the band corresponding to the TG-rich fraction suggestive of the inherent heterogeneity in particle size within VLDL. Furthermore, as illustrated in Fig. 3C, we would require a minimum concentration of 50 mg/dL of cholesterol in the TG-rich lipoprotein fraction to visualize these bands. This would correspond to a VLDL-TG in the range of 250–300 mg/dL. It is our experience that VLDL from hypertriglyceridemic plasma samples (TG $>$ 300 mg/dL) do not enter the gel gradient. This is not unexpected as from the gel constant and equation 6 we can demonstrate that, in theory, only particles less than 55.9 nm would be expected to enter the 2% gel at the top of the gradient.

Using HDL fractions that have been isolated by immunoaffinity chromatography, we have been able to demonstrate a high correlation between estimates of particle size obtained using the protein-stained SFBR 3/31 gels and the particle diameters obtained with our lipid-stained segmental gradient gel (r = 0.978). The slope of the regression line, however, is only 0.59, with our approach using the lipid stain giving a higher estimate of particle diameter. Once we adjusted the diameters of the HDL subfractions in our calibrator, the two gel systems gave identical results (Fig. 6B).

In non-denaturing gradient gel electrophoresis, it is expected that the pore size matrix will determine to which location a particle of a given diameter will migrate. In preliminary studies, we noted that the migration distances of HDL_2 and HDL_3 were not different between runs of 8, 16, and 24 h (data not presented). For LDL and Lp[a], however, a run time of 8 h or less was not adequate to define the true diameter for LDL and Lp[a]. There was no difference in the migration distance for LDL and Lp[a] when the electrophoresis was allowed to continue to 24 h (data not presented). Attempts to shorten the run time by varying the voltage or current have typically resulted in cracks in the gel by the end of the electrophoresis.

A new concept introduced in this report is the use of the parameter defined as the gel constant to characterize a linear gradient, thus allowing for better standardization among gels. The conventional approach which uses molecular weight for the estimation of particle diameter is based on a relation between the volume of a particle and the density of the fraction. The gel constant is defined by the particle size of the calibrator and the polyacrylamide concentrations in the gradient. For this approach to work, the electrophoresis protocol must be allowed to proceed slowly to complete equilibrium. The fact that the same identical gel constant (113.5 for the 2–8% gradient and 116.4 for the 8–30% gradient) was obtained for over 100 gradient gels prepared individually over a 12-month period would provide indirect support that the reported conditions are optimal for the reproducibility of these gels. While the R_f approach requires the interpolation of particle size from a number of calibrators of known diameters, the gel constant approach allows the determination of a unique gel constant that is characteristic of the acrylamide gradient formed. The diameter of the unknown particle can be directly calculated from the gel constant and the distance of the desired band from the top of the gel without referring back to a standard curve based on known calibrators. The reproducibility of the gel constant derived from the same set of calibrators can be used as a quality control for the gel gradients.

The development of this system was supported in part by a start-up grant from the Department of Medicine at the Emory University School of Medicine to the Division of Arteriosclerosis & Lipid Metabolism and the Emory Lipid Research Laboratory. The authors are indebted to Dr. Marian Cheung for the HDL subfractions which were generously donated for

comparison purposes and for her comments in the preparation of the final manuscript.

Manuscript received 7 March 1996, in revised form 27 January 1997, and in re-revised form 4 September 1997.

REFERENCES

1. Fisher, W. R., M. G. Hammond, M. C. Mengel, and G. L. Warmke. 1975. A genetic determinant of the phenotypic variance of the molecular weight of low density lipoprotein. *Proc. Natl. Acad. Sci. USA.* **72:** 2377–2351.
2. Shen, M. M. S., R. M. Krauss, F. T. Lindgren, and T. M. Forte. 1981. Heterogeneity of serum low density lipoproteins in normal human subjects. *J. Lipid Res.* **22:** 236–277.
3. Austin, M. A., and R. M. Krauss. 1986. Genetic control of low density lipoprotein subclasses. *Lancet.* **2:** 592–595.
4. Austin, M. A., J. L. Breslow, C. H. Hennekens, C. E. Buring, W. C. Willett, and R. M. Krauss. 1988. Low-density lipoprotein subclass patterns and risk of myocardial infarction. *J. Am. Med. Assoc.* **260:** 1917–1921.
5. Austin, M. A., M. C. King, K. M. Vranizan, B. Newman, and R. M. Krauss. 1988. Inheritance of low-density lipoprotein subclass patterns: results of complex segregation analysis. *Am. J. Hum. Genet.* **73:** 838–876.
6. Campos, S., J. J. Genest, Jr., E. Blijlevens, J. R. McNamara, J. L. Jenner, J. M. Ordovas, P. W. F. Wilson, and E. J. Schaefer. 1992. Low density lipoprotein particle size and coronary artery disease. *Arterioscler. Thromb.* **12:** 187–195.
7. Coresh, J., P. O. Kwiterovich, H. H. Smith, and P. S. Bachorik. 1993. Association of plasma triglyceride concentration and LDL particle diameter, density, and chemical composition with premature coronary artery disease in men and women. *J. Lipid Res.* **37:** 1687–1697.
8. Cheung, M. C., B. G. Brown, A. C. Wolf, and J. J. Albers. 1991. Altered particle size distribution of apoA-I-containing lipoproteins in subjects with coronary artery disease. *J. Lipid Res.* **32:** 383–397.
9. Johansson, J., L. A. Carlson, C. Landou, and A. Hamsten. 1991. High density lipoproteins and coronary atherosclerosis: a strong inverse relation with the largest particles is confined to normotriglyceridemic patients. *Arterioscler. Thromb.* **11:** 177–182.
10. Blanche, P. J., E. L. Gong, T. M. Forte, and A. V. Nichols. 1981. Characterization of human high density lipoproteins by gradient gel electrophoresis. *Biochim. Biophys. Acta.* **665:** 708–719.
11. Rainwater, D. L., D. W. Andres, A. L. Ford, W. F. Lowe, P. J. Blanche, and R. M. Krauss. 1992. Production of polyacrylamide gradient gels for the electrophoretic resolution of lipoproteins. *J. Lipid Res.* **33:** 1876–1881.
12. Singh, A. T. K., D. L. Rainwater, S. M. Haffner, J. L. Vandeberg, W. R. Shelledy, P. H. Moore, Jr., and T. D. Dyer. 1995. Effects of diabetes on lipoprotein size. *Arterioscler. Thromb. Vasc. Biol.* **15:** 1805–1811.
13. Gambert, P., C. Bouzerand-Gambert, A. Athias, M. Farnier, and C. Lallemant. 1990. Human low density lipoprotein fractions separated by gradient gel electrophoresis: composition, distribution, and alterations induced by cholesteryl ester transfer protein. *J. Lipid Res.* **31:** 1199–1210.
14. Fawcett, J. S., and C. J. O. R. Morris. 1966. Molecular sieve chromatography of proteins on granulated polyacrylamide gels. *Sep. Sci.* **1:** 9–26.
15. Andrews, A. T. 1986. Electrophoresis, Oxford Science Publications, New York. 7–8.
16. Haffner, S. M., X. Li, M. P. Stern, and B. V. Howard. 1992. Epidemiological correlates of LDL subfractions in the San Antonio Heart Study. *Circulation.* **86:** I-812 (Abstract).
17. Haffner, S. M., L. Mykkanen, R. A. Valdez, M. Paidi, M. P. Stern, and B. V. Howard. 1993. LDL size and subclass pattern in a biethnic population. *Arterioscler. Thromb.* **13:** 1623–1630.
18. Fless, G. M., M. E. ZumMallen, and A. M. Scanu. 1986. Physico-chemical properties of apolipoprotein[a] and lipoprotein[a−] derived from the dissociation of human lipoprotein[a]. *J. Biol. Chem.* **261:** 8712–8718.
19. Ruotolo, G., H. Zhang, V. Bentsianov, and N-A. Le. 1992. Protocol for the study of the metabolism of retinyl esters in plasma lipoproteins during postprandial lipemia. *J. Lipid Res.* **33:** 1541–1549.
20. Le, N-A., P. M. Coates, P. R. Gallagher, and J. A. Cortner. 1997. Kinetics of retinyl esters during postprandial lipemia in man: a compartmental model. *Metabolism.* **46:** 584–594.
21. Evans, G. F., W. R. Bensch, L. D. Apelgren, D. Bailey, R. F. Kaufman, T. F. Bumol, and S. H. Zuckerman. 1994. Inhibition of cholesteryl ester transfer protein in normocholesterolemic and hypercholesterolemic hamsters: effect of HDL subspecies, quantity, and apolipoprotein distribution. *J. Lipid Res.* **35:** 1634–1645.